ELSEVIER

Journal of Alloys and Compounds 404–406 (2005) 570–575

Journal of ALLOYS AND COMPOUNDS

www.elsevier.com/locate/jallcom

TEM study of the dislocations generated by hydrogen absorption/desorption in $LaNi_5$ and derivatives

B. Décamps[a,*], J.-M. Joubert[a], R. Cerny[b], A. Percheron-Guégan[a]

[a] *Laboratoire de Chimie Métallurgique des Terres Rares, CNRS, 2-8 rue Henri Dunant, 94320 Thiais Cedex, France*
[b] *Laboratoire de Cristallographie, Université de Genève, 24 quai E. Ansermet, 1211 Genève 4, Suisse*

Received 6 September 2004; accepted 7 December 2004
Available online 14 July 2005

Abstract

The combination of bright-field and weak-beam transmission electron microscopy (TEM) techniques has been used to analyse the dislocation systems activated in $LaNi_5$ and derivatives after hydrogen absorption/desorption cycling. The TEM results are discussed and compared with those obtained from the modelling of the anisotropic diffraction peak broadening using only two dislocation slip systems of the hexagonal structure.

Keywords: Electrode materials; Hydrogen storage materials; Scanning and transmission electron microscopy; Dislocations and disclinations; X-ray diffraction

1. Introduction

$LaNi_5$ and its substitutional derivatives which are commonly used for hydrogen storage are commercially developed in nickel-metal hydride (Ni-MH) batteries. During absorption/desorption cycling, dislocations are produced as a consequence of the interaction of hydrogen with the material. After cycling, $LaNi_5$ exhibits an intense anisotropic diffraction peak broadening that can be reduced in substitutional compounds [1–3]. This broadening has been studied in $LaNi_5$ by means of neutron powder diffraction [4], and in $LaNi_5$ and some derivatives, by means of synchrotron powder diffraction [5]. By modelling it, using the theory developed by Krivoglaz [6] and the procedure described by Klimanek et al. [7] for the hexagonal system (Table 1), with only two slip systems of the hexagonal structure (E1 and E2), it has been possible to estimate the dislocation density for each studied compound together with the ratio E1/E2 [5]. Such systems together with c-type dislocations have been identified by transmission electron microscopy (TEM) in $LaNi_5$ either deformed [8] or hydrogenated [9,10]. Nevertheless, a combination of other systems cannot be excluded. So, it is essential to determine by transmission electron microscopy (TEM) which systems are activated depending upon the substitution. Several intermetallic compounds studied by X-ray diffraction have been chosen for the TEM study as they present different dislocation densities and E1/E2 ratios. Dislocation analyses are performed using bright-field and weak-beam techniques. The results are then compared and discussed with those obtained by X-ray diffraction on the same compounds.

2. Experimental

The intermetallic compounds ($LaNi_5$ and substitutional derivatives containing Co, Mn and Al) were synthesised by induction melting of the pure elements followed by a suitable annealing [5]. Their single-phase character and compositional homogeneity were checked by X-ray diffraction (XRD), optical metallography and electron probe microanalysis. They crystallise in the hexagonal structure of $CaCu_5$ type (space group $P6/mmm$ with La in 1*a* (0 0 0) and Ni in 2*c* (1/3 2/3 0) and 3*g* (1/2 0 1/2)). Fifteen absorption/desorption cycles were conducted at 313 K on crushed

* Corresponding author. Tel.:+33 1 49 78 12 14; fax: +33 1 49 78 12 03.
E-mail address: brigitte.decamps@glvt-cnrs.fr (B. Décamps).

0925-8388/$ – see front matter © 2005 Elsevier B.V. All rights reserved.
doi:10.1016/j.jallcom.2004.12.162

Table 1
Dislocations and slip systems considered in hexagonal materials [7]

Dislocation	Type	Burgers vector	Slip type	Slip plane
S1	Screw	1/3 ⟨−2, 1, 1, 0⟩	–	–
S2	Screw	⟨0 0 0 1⟩	–	–
S3	Screw	1/3 ⟨−2, 1, 1, 3⟩	–	–
E1	Edge	1/3 ⟨−2, 1, 1, 0⟩	Basal	{0 0 0 1}
E2	Edge	1/3 ⟨−2, 1, 1, 0⟩	Prismatic	{0,−1,1,0}
E3	Edge	⟨0 0 0 1⟩	Prismatic	{0,−1,1,0}
E4	Edge	1/3 ⟨−2, 1, 1, 3⟩	Prismatic	{0,−1,1,0}
E5	Edge	1/3 ⟨−2, 1, 1, 0⟩	Pyramidal	{0,−1,1,1}
E6	Edge	1/3 ⟨−2, 1, 1, 3⟩	Pyramidal	{0,−1,1,1}
E7	Edge	1/3 ⟨−2, 1, 1, 3⟩	Pyramidal	{1,1,−2,1}
E8	Edge	1/3 ⟨−2, 1, 1, 3⟩	Pyramidal	{2,−1,−1,2}

samples. Six cycled compounds studied by X-ray diffraction [5] have been chosen for the TEM study as they present different dislocation densities and E1/E2 ratios (Table 2). TEM specimens were prepared by cold rolling a mixture of the compound, reduced into powder by decrepitation during cycling, with Al powder. Three millimeters discs were then punched out and ion milled to perforation using a precision ion polishing system (PIPS) with 4–2 keV Ar^+ ion at an incidence angle of 5°. The samples were observed in JEOL 2000EX and FX transmission electron microscopes. Micrographs were taken under bright-field [11] and weak-beam conditions [12]. Burgers vector analysis was performed using the invisibility criterion $\mathbf{g} \cdot \mathbf{b} = 0$ [13]. When possible, the dislocation line direction **u** has been determined by trace analysis. For convenience, Table 3 gives the equivalence between the four indices notation of the hexagonal system (useful to represent the equivalent orientations) and the three indices one used for crystallographic calculations (such as $\mathbf{g} \cdot \mathbf{b}$ calculations) for all Burgers vectors of Table 1.

3. Results

The results of the TEM analysis are summarized for the six studied compounds in Table 2. Only the detailed TEM analysis of $LaNi_5$, $LaNi_{4.6}Mn_{0.4}$ and $LaNi_{3.94}Co_{0.36}Mn_{0.4}Al_{0.3}$ compounds is given in this paper. The detailed results for the other compounds, $LaNi_{4.25}Co_{0.75}$, $LaNi_4Mn$ and $LaNi_{3.55}Co_{0.75}Mn_{0.4}Al_{0.3}$, are given in Ref. [14].

3.1. $LaNi_5$

The TEM study reveals the presence of many dislocations in the thin foil as shown in Fig. 1. These dislocations are visible for $\mathbf{g} = -2, 2, 0$ (Fig. 1a) and out of contrast for $\mathbf{g} = 0, 0, -2$ (Fig. 1b) which means that their Burgers vector is equal to **a** ($\mathbf{b} = 1/3\langle -2, 1, 1, 0\rangle$). As these dislocations are aligned close to $\mathbf{u} = [0\,0\,0\,1]$, they belong to the slip system E2. The dislocation density can be estimated to be in the range $10^{11}\,cm^{-2}$. The observations do not reveal the presence of **a**-type dislocations lying in the basal plane so the E1 slip system has not been evidenced. On the other hand, many dislocations are visible for $\mathbf{g} = 0, 0, -2$ which indicates that their Burgers vector is different of **a**. A few of them are clearly out of contrast for $\mathbf{g} = -2, 2, 0$. This shows that their Burgers vector is equal to **c** ($\mathbf{b} = [0\,0\,0\,1]$). A few of them are screw as their line direction is close to $\mathbf{u} = [0\,0\,0\,1]$. For most of these dislocations, it has not been possible to determine precisely their orientation due to the curvature of their line.

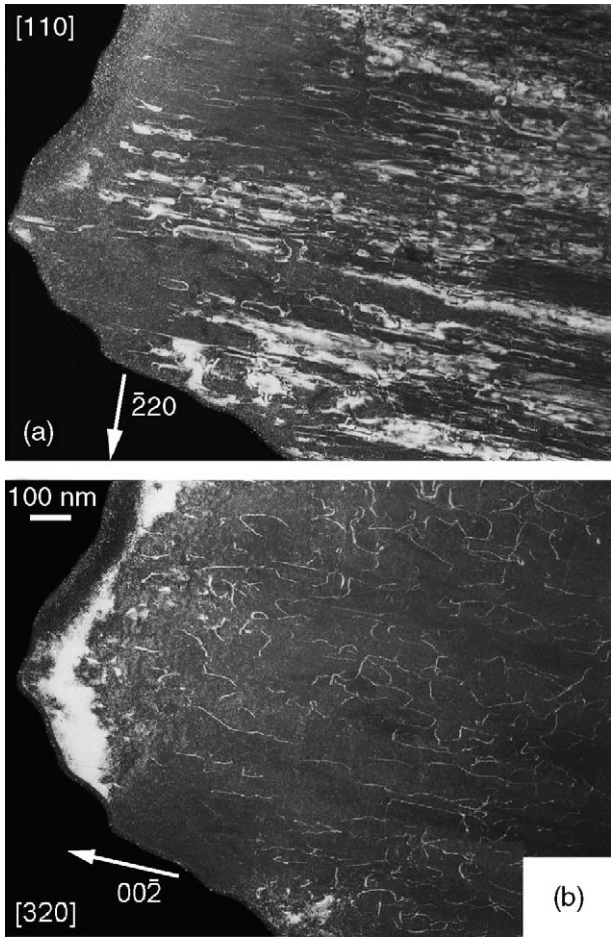

Fig. 1. $LaNi_5$ compound after 15 hydrogen absorption/desorption cycles. Weak-beam micrographs ((a) and (b)) taken in two different orientations.

Table 2
Results of the X-ray diffraction peak broadening modelling using E1 and E2 (lattice parameters after cycling, dislocation density and dislocation fractions E1 and E2) [5] and results of the TEM analysis for all the compounds

Compound	X-ray modelling [5]			TEM analysis
	Dislocation density (10^{11} cm^{-2})	E1 (%)	E2 (%)	
$LaNi_{4.25}Co_{0.75}$	3.9	2	98	Long dislocations with $b = 1/3\langle -2, 1, 1, 0\rangle$ and $u = 0\,0\,0\,1$: E2 system. Very few dislocations with $b \neq 1/3\langle -2, 1, 1, 0\rangle$
$LaNi_5$	3.8	11	89	Long dislocations with $b = 1/3\langle -2, 1, 1, 0\rangle$ and $u = [0\,0\,0\,1]$: E2 system. Numerous dislocations with $b \neq 1/3\langle -2, 1, 1, 0\rangle$: $\neq$ E1 and E2 systems. A few dislocations with $b = \langle 0\,0\,0\,1\rangle$. Dislocation density in the range 10^{11} cm^{-2}
$LaNi_{4.6}Mn_{0.4}$	2.7	36	64	Long dislocations with $b = 1/3\langle -2, 1, 1, 0\rangle$ and $u = 0\,0\,0\,1$: E2 system. A few dislocations with $b = \langle 0\,0\,0\,1\rangle$
$LaNi_4Mn$	3.8	64	36	Dislocations with $b = 1/3\langle -2, 1, 1, 3\rangle \neq$ E1 and E2 systems, possibly belonging to the E7 system. Dislocation bands composed of several Burgers vectors possibly lying in basal or pyramidal planes
$LaNi_{3.94}Co_{0.36}Mn_{0.4}Al_{0.3}$	1.7	79	21	Long dislocations with $b = 1/3\langle -2, 1, 1, 0\rangle$. Probably E2 system. Dislocations with $b = 1/3\langle 1, -2, 1, 3\rangle \neq$ E1 and E2 systems, possibly belonging to the E7 system
$LaNi_{3.55}Co_{0.75}Mn_{0.4}Al_{0.3}$	0.17	92	8	Very few dislocations

Table 3
Correspondence between the four and three indices notation for the Burgers vectors of dislocations of Table 1

a-Type dislocations: $1/3[2, -1, -1, 0] = [1\,0\,0]$, $1/3[1, 1, -2, 0] = [1\,1\,0]$, $1/3[-1, 2, -1, 0] = [0\,1\,0]$
c-Type dislocation: $[0\,0\,0\,1] = [0\,0\,1]$
Other dislocations: $1/3[2, -1, -1, 3] = [1\,0\,1]$, $1/3[1, 1, -2, -3] = [1, 1, -1]$, $1/3[-1, 2, -1, 3] = [0\,1\,1]$, $1/3[-2, 1, 1, 3] = [-1, 0, 1]$, $1/3[1, 1, -2, 3] = [1\,1\,1]$, $1/3[1, -2, 1, 3] = [0, -1, 1]$

3.2. $LaNi_{4.6}Mn_{0.4}$

Many dislocations are present in the compound (Fig. 2). A few dislocations denoted A have their Burgers vector equal to **c** as they are visible for $\mathbf{g} = 0\,0\,2$ (Fig. 2a) and out of contrast for $\mathbf{g} = 0, -2, 0$ (Fig. 2b) and $\mathbf{g} = -1, 2, 0$ (not presented here). Many long dislocations (noted B on Fig. 2b), aligned along the $[0\,0\,0\,1]$ direction, out of contrast for $\mathbf{g} = 0\,0\,2$ and visible for $\mathbf{g} = 0, -2, 0$, belong to the E2 slip system.

3.3. $LaNi_{3.94}Co_{0.36}Mn_{0.4}Al_{0.3}$

Two dislocation family are observed in the compound. One is consistent with the E2 slip system (Fig. 3) with dislocations out of contrast for $\mathbf{g} = 0\,0\,2$ (Fig. 3a) and visible for $\mathbf{g} = -2, 2, 0$ (Fig. 3b) and dislocation line close to $\mathbf{u} = [0\,0\,0\,1]$. The second dislocation family denoted A in Fig. 4 has a Burgers vector equal to $\mathbf{c} + \mathbf{a}$. Dislocations are visible for $\mathbf{g} = 2, -2, 0$ (Fig. 4a) and out of contrast for $\mathbf{g} = 1, -1, -1$ (Fig. 4b) which is consistent with $\mathbf{b} = 1/3$ [2,−1,−1,3] or $\mathbf{b} = 1/3$ [1,−2,1,3]. Their dislocation line orientation, although difficult to precisely determine in this case, strongly suggests that they belong to the E7 slip system (1/3 [1,−2,1,3](2,−1,−1,1)) for the edge character to be favored.

4. Discussion

The combination of bright-field and weak-beam TEM techniques has been used to analyse the dislocation characteristics generated during hydrogen absorption/desorption cycles in $LaNi_5$ and derivatives. Such a study is complementary to that presented earlier on four compounds [14].

The first point to discuss is the validity of the TEM analysis as the thin foil preparation technique is different from those commonly used in the literature for this type of compounds [8–10,15–17]. In our technique, powders are cold rolled with aluminium to obtain thin foils about 100 μm thick. Such a technique is commonly used to obtain 3 mm disks from powder materials but dislocations could have been introduced during this process. This is not the case as hardly any dislocations were observed in the $LaNi_{3.55}Co_{0.75}Mn_{0.4}Al_{0.3}$ compound. So the observed microstructure is readily that produced during hydrogen cycling for all the compounds.

The next point to address is the comparison between TEM results and those given by the anisotropic peak broadening modelling [5] as the observed compounds are coming from the same batch. Six compositions were chosen depending upon the dislocation density and the E1/E2 ratio. The comparison is easily done looking at Table 2. The results are in perfect agreement for two compounds: $LaNi_{3.55}Co_{0.75}Mn_{0.4}Al_{0.3}$ and $LaNi_{4.25}Co_{0.75}$. For the first one, the TEM observation reveals an extremely low dislocation density, consistent with the strong reduction of anisotropic peak broadening related to the absence of dislocation activity. Nevertheless, the calculated density coming from the X-ray experiment [5] and reported in Table 2 should give rise to a larger deformation in TEM experiments. Such result is linked to the difficulty to measure low density of defects by X-ray experiments. The second compound, according to the X-ray experiment should present a high density of only **a**-type dislocations belonging

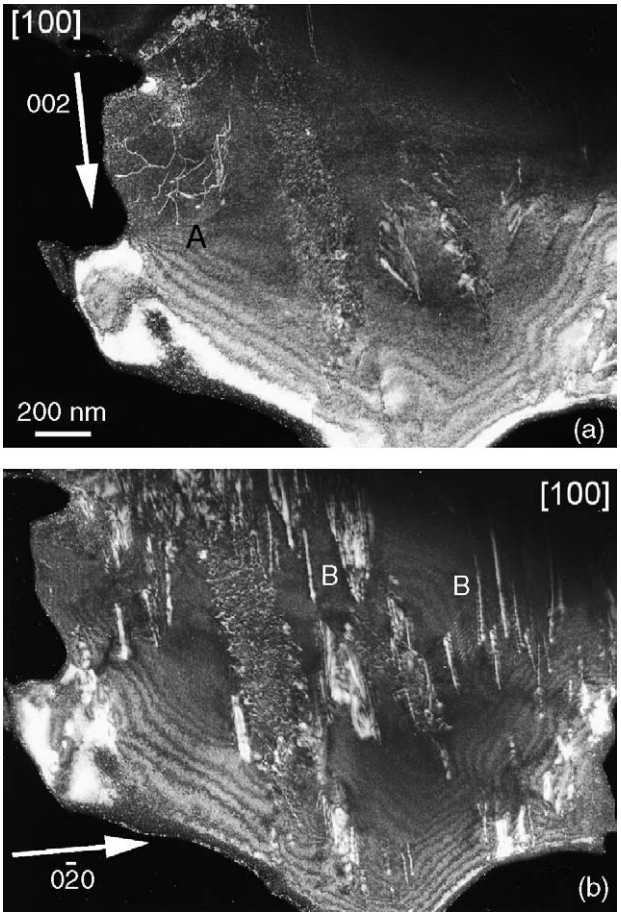

Fig. 2. $LaNi_{4.6}Mn_{0.4}$ compound after 15 hydrogen absorption/desorption cycles. Weak-beam micrographs ((a) and (b)) taken in two different orientations. Two dislocation families (A and B) are indicated on micrographs.

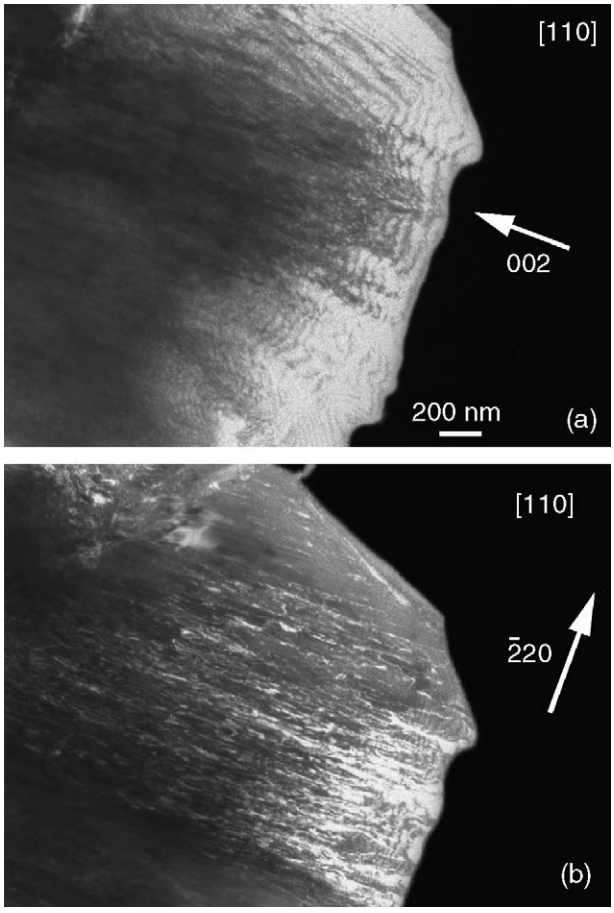

Fig. 3. $LaNi_{3.94}Co_{0.36}Mn_{0.4}Al_{0.3}$compound after 15 hydrogen absorption/desorption cycles. Weak-beam ((a) and (b)) micrographs taken in two different orientations.

to the E2 glide system. The TEM study confirms that point, as numerous dislocations with **a**-type Burgers vector are observed within the sample and no other system seems to be activated. For $LaNi_5$ and $LaNi_{4.6}Mn_{0.4}$, the peak broadening modelling (Table 2) predicted a high density of dislocations with an E1/E2 ratio of 11/89 and 36/64 respectively. If the TEM analysis reveals the presence of dislocations belonging to the E2 system in both case (Table 2), the E1 system has not been evidenced. Such an activation of the E2 system is very consistent with what has been previously observed by TEM in the literatures [16,17] in $LaNi_5$ but only after one hydrogen absorption/desorption cycle. A density of the order 10^{12} to 10^{13} cm^{-2} has been estimated in the literature in $LaNi_5$, after only one cycle of hydrogen absorption/ desorption, either by X-ray experiment [18] or TEM observations [17]. Such values appear higher than what can be estimated from our TEM analysis (range consistent with the value obtained from synchrotron experiment [5] – see Table 2). Furthermore, the presence of other dislocations such as **c**-type dislocations has been shown: a few of them have a screw orientation. Such dislocations moving on prismatic planes may be emitted from cracks in $LaNi_5$ [8], they could be produced during the compound decrepitation produced by hydrogen cycling. Their motion should be easier than that of **a**-type dislocations [8]. The $LaNi_4Mn$ compound exhibits a different behaviour at the TEM level (Table 2) from that predicted by the anisotropic peak modelling [5]. According to Table 2, the presence of a large density of dislocations in a ratio E1/E2 of 64/36 was expected in this sample. In this case, neither of these two systems has been clearly identified. Dislocation bands composed of different Burgers vectors have been observed: they could glide either in the basal plane or in a pyramidal plane, which means that the E1 system could be one of the activated system but not the E2 one. The TEM analysis reveals also the presence of another activated system (possibly E7) not taken into account in the modelling. The last compound $LaNi_{3.94}Co_{0.36}Mn_{0.4}Al_{0.3}$ compound, with expected E1/E2 ratio of 79/21 exhibits two sets of dislocations. One is the expected E2 slip system while the other (probably E7) is different from the E1 system.

So, as a quick conclusion about this comparison, it can be noted that the E2 system has been generally observed in all concerned compounds except for $LaNi_4Mn$, while E1 has never been evidenced even in compounds with expected high E1 density such as $LaNi_4Mn$ and $LaNi_{3.94}Co_{0.36}Mn_{0.4}Al_{0.3}$. In these cases, another slip system (probably E7) is strongly

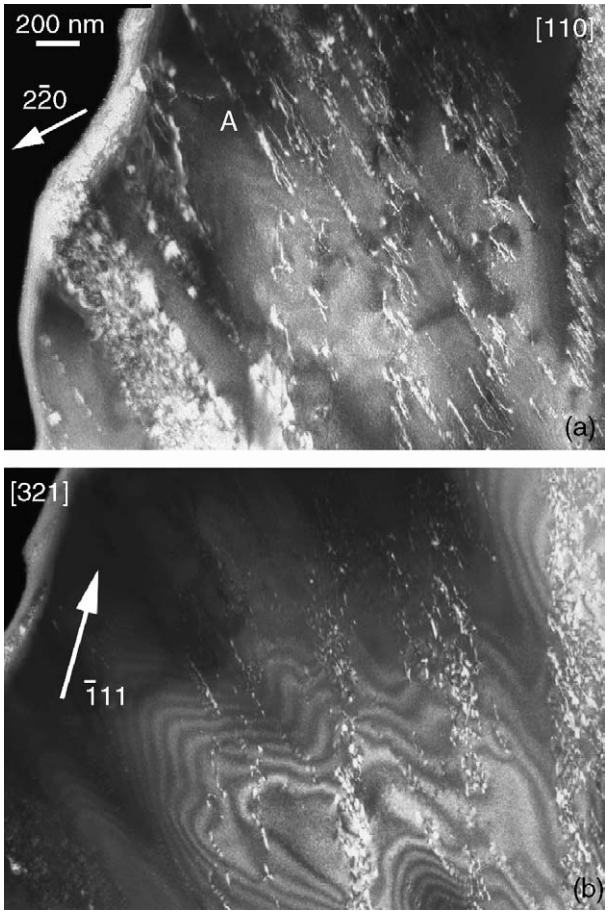

Fig. 4. $LaNi_{3.94}Co_{0.36}Mn_{0.4}Al_{0.3}$compound after 15 hydrogen absorption/desorption cycles. Weak-beam ((a) and (b)) micrographs taken in two different orientations. A indicates the analysed dislocation family.

activated. Such result leads to a discussion about the systems involved in the modelling [5]. Fig. 5 displays the calculated diffraction line broadening for all slip systems of the hexagonal structure [7]. From Fig. 5, the implication of E2 explains the strong broadening of $h\,k\,0$ peaks and the absence of broadening of 0 0 l peaks. For $LaNi_4Mn$, which presents, on contrary to the other samples, a strong broadening of 0 0 l lines, another system had to be considered. As numerous systems could be responsible for the broadening (see Fig. 5), E1 system was chosen among others because of the following reasons: The E5 system has been excluded as, used in combination with E2, it did not explain the behaviour of the peak broadening: strongly anisotropic ($LaNi_5$) to nearly isotropic ($LaNi_4Mn$). Other systems such as E4, E6, E7 or E8 had been excluded, as they were never observed in previous TEM studies in cycled [9,10,16,17] or non-cycled [8] $LaNi_5$. However, the presence of these systems is not in contradiction with the X-ray results [5] especially because, if combined with E2, it could explain an isotropic broadening as observed in e.g. $LaNi_4Mn$. The present study reveals the possible activation of other systems as maybe E7. They should probably be taken into account in the modelling of compounds presenting a strong broadening of 0 0 *l* lines.

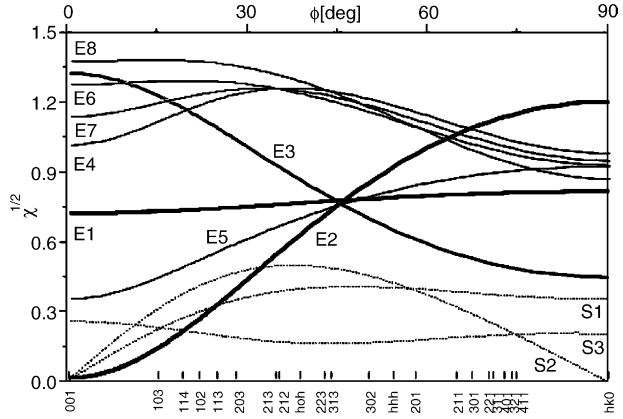

Fig. 5. Calculated diffraction line broadening behaviour as a function of $h\,k\,l$, for the different slip systems of the hexagonal structure [7].

This study clearly demonstrates the complementarity of the TEM and X-ray techniques for the analysis of defects. While the first technique is accurate for low defect density measurement, the second one is more appropriate for high dislocation density estimation. Moreover, such a combination yields a complete description of the sample behaviour at microscopic and macroscopic scales.

5. Conclusion

The TEM analysis, which allows to visualize the true sample microstructure, is in good agreement with the activation of the E2 system for most compounds and the absence of dislocation activity in $LaNi_{3.55}Co_{0.75}Mn_{0.4}Al_{0.3}$. However the activation of the E1 system is never demonstrated. Instead, the activation of another system (probably E7) is evidenced for compounds modelled with a high E1 density.

Such an analysis demonstrates that diffraction line broadening modelling using only E1 and E2 is probably not accurate and that other systems should be taken into account.

Acknowledgement

The authors wish to thank V. Lalanne for the TEM specimen preparation.

References

[1] A. Percheron-Guégan, C. Lartigue, J.-C. Achard, P. Germi, F. Tasset, J. Less-Common Met. 74 (1980) 1.
[2] S.W. Lambert, D. Chandra, W.N. Cathey, F.E. Lynch, R.C. Bowman Jr., J. Alloys Compd. 187 (1992) 113.
[3] J.-M. Joubert, R. Cerny, M. Latroche, A. Percheron-Guégan, K. Yvon, J. Alloys Compd. 265 (1998) 311.
[4] E. Wu, F.H. Kisi, E.MacA. Gray, J. Appl. Crystallogr. 31 (1998) 363.
[5] R. Cerny, J.-M. Joubert, M. Latroche, A. Percheron-Guégan, K. Yvon, J. Appl. Cryst. 33 (2000) 997.

[6] M.A. Krivoglaz, Theory of X-Ray and Thermal Neutron Scattering by Real Crystals, Plenum Press, New York, 1969.
[7] P. Klimanek, R. Jr. Kuzel, J. Appl Crystallogr. 21 (1988) 59–66, 363–368.
[8] H. Inui, T. Yamamoto, Z. Di, M. Yamaguchi, J. Alloys Compd. 269 (1998) 294.
[9] G.-H. Kim, C.-H. Chun, S.-G. Lee, J.-Y. Lee, Acta Metall. Mater. 42 (9) (1994) 3157.
[10] G.-H. Kim, S.-G. Lee, K.-Y. Lee, C.-H. Chun, J.-Y. Lee, Acta Metall. Mater. 43 (6) (1995) 2233.
[11] P.B. Hirsch, A. Howie, R.B. Nicholson, D.W. Pashley, M.J. Whelan, Electron Microscopy of Thin Crystals, Krieger, New York, 1977.
[12] D.J.H. Cockayne, I.L.F. Ray, M.J. Whelan, Phil. Mag. 20 (1969) 1265.
[13] A. Howie, M.J. Whelan, Proc. Roy. Soc. A 267 (1962) 206.
[14] B. Décamps, J.-M. Joubert, R. Cerny, A. Percheron-Guégan, Mater. Res. Soc. Symp. Proc. 753 (2003) 509.
[15] A.E.M. de Weirman, A.A. Staals, P.H.L. Notten, Phil. Mag. A 70 (5) (1994) 837.
[16] T. Yamamoto, H. inui, M. Yamaguchi, Mater. Sci. Eng. A 329/331 (2002) 367.
[17] H. Inui, T. Yamamoto, M. Hirota, M. Yamaguchi, J. Alloys Compd. 330/332 (2002) 117.
[18] E. Wu, E.MacA. Gray, D.J. Cookson, J. Alloys comp. 330/332 (2002) 229.